

Supporting Information

Asymmetric yolk@shell structured Fe-doped polydopamine or carbon@mesoporous silica composite particles

Baorui Liang, Ruonan Ouyang, Wenchao Li, Haodong Guo, Junjie Liu, Xin Du*

Baorui Liang, Junjie Liu

Tianjin College, University of Science and Technology Beijing, Tianjin 301830,
China

Ruonan Ouyang, Wenchao Li, Haodong Guo, Prof. Xin Du

Beijing Key Laboratory for Bioengineering and Sensing Technology, School of
Chemistry and Biological Engineering, University of Science and Technology
Beijing, Beijing 100083, China

*E-mail: duxin@ustb.edu.cn

1. Reagents and materials

Reagents and characterization are placed in Supporting Information. Dopamine hydrochloride (DA·HCl, 99%), cetyltrimethylammonium chloride (CTAC, 99%), and tris(hydroxymethyl)aminomethane (tris, 99%) were purchased from Adamas. Aqueous ammonia (NH₃·H₂O, 25-28 %) was purchased from Sinopharm. Anhydrous ethanol (99.9%) was bought from Beijing Chemical Industry. Tetraethyl orthosilicate (TEOS, 99.9%) and triethanolamine (TEA, 99%) were obtained from Sigma-Aldrich. Hydrogen peroxide (H₂O₂, 30 wt%) aqueous solution, ferric chloride hexahydrate (FeCl₃·6H₂O) and doxorubicin hydrochloride (DOX·HCl) were bought from Aladdin reagent Co., Ltd. (Shanghai, China). Methylene blue (MB) was bought from Sinopharm Chemical Reagent Co., Ltd. All chemicals were used directly without any further purification. Ultrapure water with a resistivity higher than 18.2 MΩ cm⁻¹ was used in all experiments and obtained from a three-stage Millipore Mill-Q Plus 185 purification system (Academic).

2. Characterization of surface morphology, chemical composition and magnetic property

Scanning electron microscopy (SEM) images were obtained using a SU8010 scanning electron microscope. Energy dispersive X-ray spectroscopy (EDS) was coupled for detecting the elemental mapping. For transmission electron microscopy (TEM) observations, samples dispersed in ethanol were deposited onto carbon-coated copper grids and subsequently examined with a HT7700 transmission electron microscope. Fourier transform infrared (FTIR) spectra in the wavenumber range of

500–4000 cm^{-1} was recorded by a Shimadzu FTIR-8400S spectrophotometer. The phase composition and valence states of the sample were analyzed by X-ray photoelectron spectroscopy (XPS, ESCALAB 250Xi). The ultraviolet-visible (UV-Vis) absorption spectrum in the range of 200–900 nm was measured using a Shimadzu UV-1800 spectrophotometer. The magnetic property was assessed using a vibrating sample magnetometer (VSM, 7404, Lakeshore, USA). The size of the prepared samples was measured using the software Nano Measurer 1.2. The particle dispersion index (PDI), hydrodynamic particle size and zeta potential of the prepared samples were measured by dynamic light scattering (DLS) (Nano ZS, Malvern Instruments, Worcestershire, UK).

3. Measurement of photothermal conversion performance

Aqueous suspensions of different samples were prepared and added to a 2.5 mL centrifuge tube. A NIR laser (wavelength: 808 nm, power: 3.14 W, light window: 3.14 cm^2) was used to irradiate the centrifuge tube for 10 minutes at a distance of approximately 20 cm between the light window and the centrifuge tube. A digital with 4-channel data logger thermometer (RDXL 4SD, Omega Engineering Inc.) with a 4-channel data logger was used to monitor temperature changes. The head of the thermometer was completely immersed in the solution. Each sample in the centrifuge tube was irradiated for 10 minutes and the temperature was recorded at 2 second intervals. To study the photothermal stability of the sample, three warming (808 nm, 10 min, 1.0 W cm^{-2}) and cooling (natural cooling to room temperature) cycle tests were performed. Infrared thermal images of the samples were captured with a thermal

imaging camera (TiS65, FLUKE, USA).

4. Fabrication of PDA nanospheres

PDA nanospheres (diameter: ca. 320 nm) were synthesized according to a previous report [1]. Typically, 1.2 mL of aqueous ammonia solution, 40 mL of ethanol, and 90 mL of water were mixed at room temperature. 0.5 g of dopamine hydrochloride was fully dissolved in 10 mL of water, and then quickly added into the above-mixed solution. The color of the solution immediately turned pale brown and gradually changed to dark brown. The reaction lasted for 30 h. The PDA nanospheres were collected and washed with water by centrifugation (11000 rpm for 3 times) and dried in air at 60 °C overnight.

[1] Minghang Qiao, Yi Xing, Lei Xie, Biao Kong, Freddy Kleitz, Xiaoyu Li, Xin Du, Temperature-regulated core swelling and asymmetric shrinkage for controllable yolk@shell structures of polydopamine@mesoporous silica nanospheres, *Small*, 2022, 18, 2205576. <https://doi.org/10.1002/smll.202205576>

5. DOX adsorption

A certain amount of doxorubicin (DOX) was dissolved in phosphate-buffered saline (PBS) buffer solution (0.01 M, pH=7.4) to prepare a DOX stock solution with a concentration of 1 mg mL⁻¹. 2 mg of Fe(III)-loaded PDA-3 or Fe(III)-loaded PDA@SiO₂-3 was added to 1 mL of PBS buffer solution, and after ultrasonic

dispersion for 10 minutes, 1 mL of the DOX stock solution was added. The total volume and DOX concentration of the resulting liquid were 2 mL and 0.5 mg mL⁻¹, respectively. At room temperature, the mixed solution was stirred at a rotation speed of 200 rpm for 4 hours. The DOX-loaded Fe(III)-loaded PDA-3 or Fe(III)-loaded PDA@SiO₂-3 was collected by centrifugation (11,000 rpm, 5 minutes) and separated from the unloaded DOX in the supernatant. The DOX-loaded Fe(III)-loaded PDA-3 or Fe(III)-loaded PDA@SiO₂-3 was washed three times with ultrapure water to ensure the removal of unloaded DOX. All supernatants were mixed, and the absorbance of the supernatant at a wavelength of 480 nm was measured. The DOX loading capacity in Fe(III)-loaded PDA-3 or Fe(III)-loaded PDA@SiO₂-3 was calculated according to the standard curve of DOX.

6. MB adsorption

1 mL of Fe(III)-loaded PDA-3 or Fe(III)-loaded PDA@SiO₂-3 nanoparticles (1 mg/mL) was mixed with 11 mL of methylene blue (MB) solution with an initial concentration of 10 µg/mL in a 20 mL glass vial. Subsequently, at room temperature, aliquots of the mixture were taken at 10, 20, 30, 60, and 120 minutes respectively, followed by centrifugation at 11,000 rpm for 5 minutes. The supernatant was then collected, and the absorbance of the MB solution was measured at 664 nm using a UV-Vis spectrophotometer.

7. Catalytic test

The ability of Fe(III)-loaded PDA-3 and Fe(III)-loaded PDA@SiO₂-3 nanoparticles to generate ·OH was evaluated based on the degradation of MB, which was monitored by the UV–Vis absorbance at 665 nm. The Fe(III)-loaded PDA-3 or Fe(III)-loaded PDA@SiO₂-3 nanoparticles (50 µg/mL) were dispersed into the mixture solution containing H₂O₂ (1.2 × 10⁻³ mM) and MB (10 µg/mL). The reaction was carried out at room temperature for specified time. Afterwards, the reaction mixture was centrifuged at 11 000 rpm for 5 min, and the absorbance spectra of the supernatant were measured using a UV–Vis spectrophotometer in the range of 500–800 nm.

8. CCK-8 method for cytotoxic test

Cell viability was assessed via the CCK-8 (Cell Counting Kit-8) assay. NIH/3T3 fibroblasts, adjusted to a density of 10⁵ cells mL⁻¹, were seeded into a 96-well plate at a volume of 100 µL per well and allowed to culture overnight. Fe(III)-loaded PDA@SiO₂-3 nanoparticles were formulated in PBS at a series of concentrations (0, 10, 20, 50, 100, 200 µg mL⁻¹), which were then added to the pre-seeded 96-well plate for a 6-hour incubation period. After this incubation, 10 µL of CCK-8 solution was dispensed into each well, and the plate was further incubated for 2 hours. A 96-well plate reader was used to measure absorbance at 450 nm; this absorbance value correlates with mitochondrial activity, serving as an indirect marker of viable cell count. To calculate cell viability, the absorbance of cells treated with Fe(III)-loaded PDA@SiO₂-3 nanoparticles was compared to that of untreated control cells, with

adjustments made to account for sample background interference. Cell survival rates were presented as the percentage of absorbance relative to the control group (cells not exposed to nanoparticles). All results represent the mean \pm standard deviation (SD) derived from at least three independent experiments, with five cell wells counted per experiment.

Table S1. Reactants and their ratios for preparing Fe(III)-loaded PDA-n (n = 1,2,3).

| Sample | DA·HCl (mg) | Tris (mg) | FeCl ₃ ·6H ₂ O (mg) | Total water volume (mL) |
|----------------------|----------------|-----------|--|----------------------------|
| Fe(III)-loaded PDA-1 | 45 | 90 | 1.3 | 150 |
| Fe(III)-loaded PDA-2 | 45 | 450 | 6.2 | 150 |
| Fe(III)-loaded PDA-3 | 45 | 1500 | 20.4 | 150 |

Table S2. Comparison of SEM-measured particle size and hydrodynamic diameter for different particles.

| Sample | Particle size from SEM (nm) | DLS hydrodynamic particle size (nm) |
|----------------------|--------------------------------|--|
| PDA | 320 | 362.7 |
| Fe(III)@PDA | 320 | 369.6 |
| Fe(III)-loaded PDA-1 | 180 | 219.4 |
| Fe(III)-loaded PDA-2 | 170 | 208.7 |
| Fe(III)-loaded PDA-3 | 300 | 311.3 |

Table S3. Preparation strategies and Fe contents of different particles.

| Sample | Fabrication strategy | Fe content (%) |
|----------------------|--------------------------------|----------------|
| PDA | No doping Fe | 0 |
| Fe(III)@PDA | Post-loading Fe | 0.96 |
| Fe(III)-loaded PDA-1 | Copolymerization (pre-loading) | 3.3 |
| Fe(III)-loaded PDA-2 | Copolymerization (pre-loading) | 7.6 |
| Fe(III)-loaded PDA-3 | Copolymerization (pre-loading) | 8.6 |

Table S4. Comparison of SEM-measured particle size and hydrodynamic diameter for different particles.

| Sample | Particle size from SEM (nm) | DLS hydrodynamic particle size (nm) |
|---------------------------------------|-----------------------------|-------------------------------------|
| PDA@SiO ₂ | 570 | 662.7 |
| Fe(III)@PDA@SiO ₂ | 570 | 707.8 |
| Fe(III)-loaded PDA-1@SiO ₂ | 300 | 402.7 |
| Fe(III)-loaded PDA-2@SiO ₂ | 300 | 387.7 |
| Fe(III)-loaded PDA-3@SiO ₂ | 490 | 510.2 |

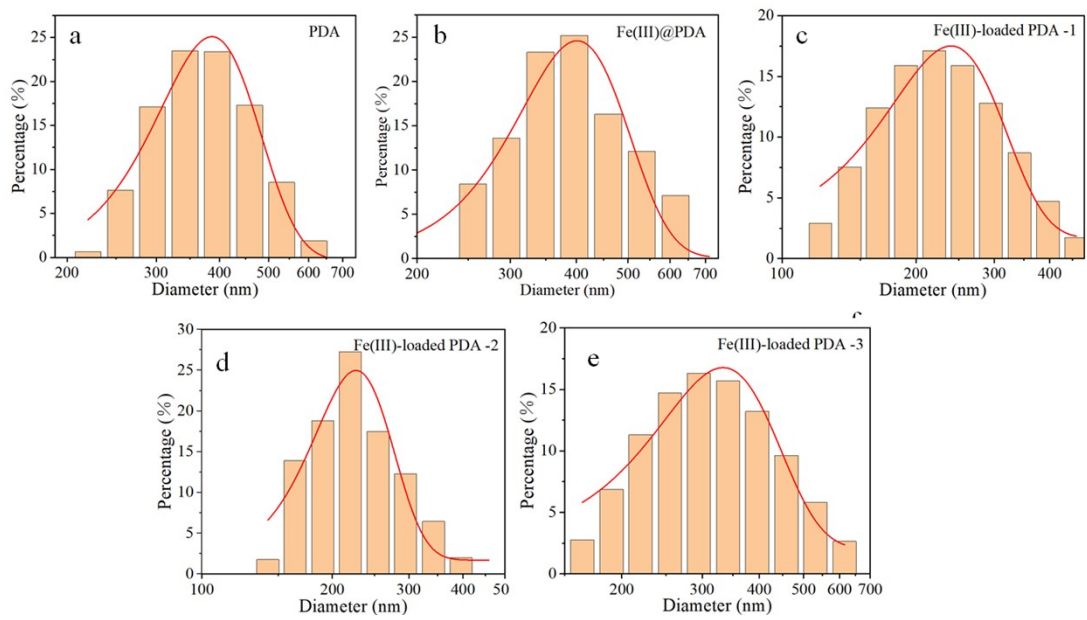


Figure S1. The diagrams of hydrodynamic particle size of (a) PDA, (b) Fe(III)@PDA, (c-e) Fe(III)-loaded PDA-(1-3).

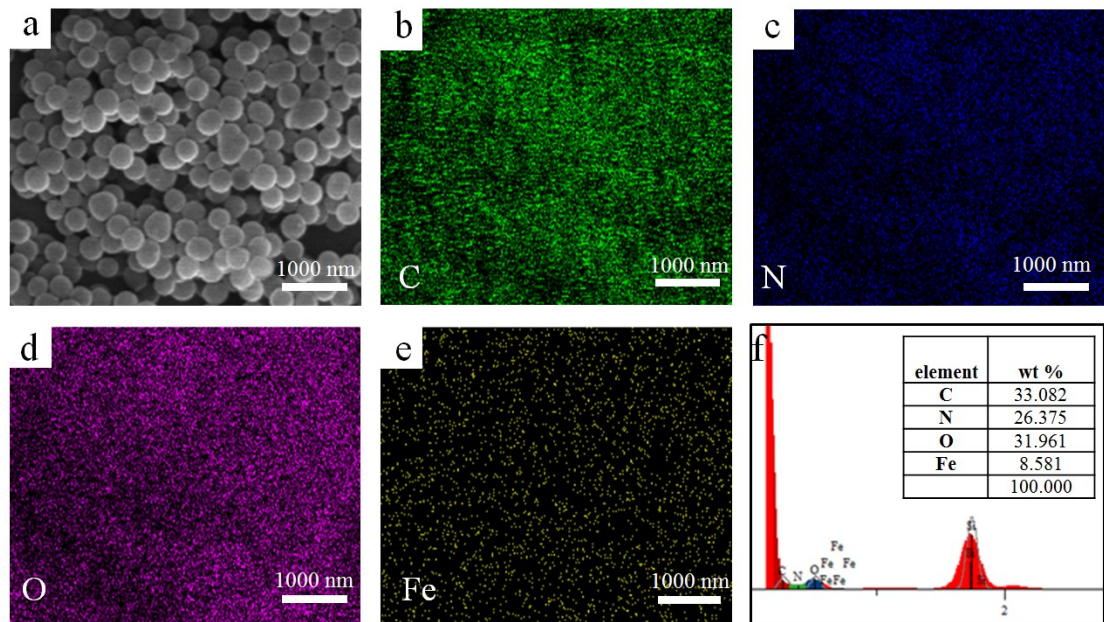


Figure S2. (a) SEM, (b-e) EDS elemental mapping images and (f) EDS spectra of Fe(III)-loaded PDA-3 particles

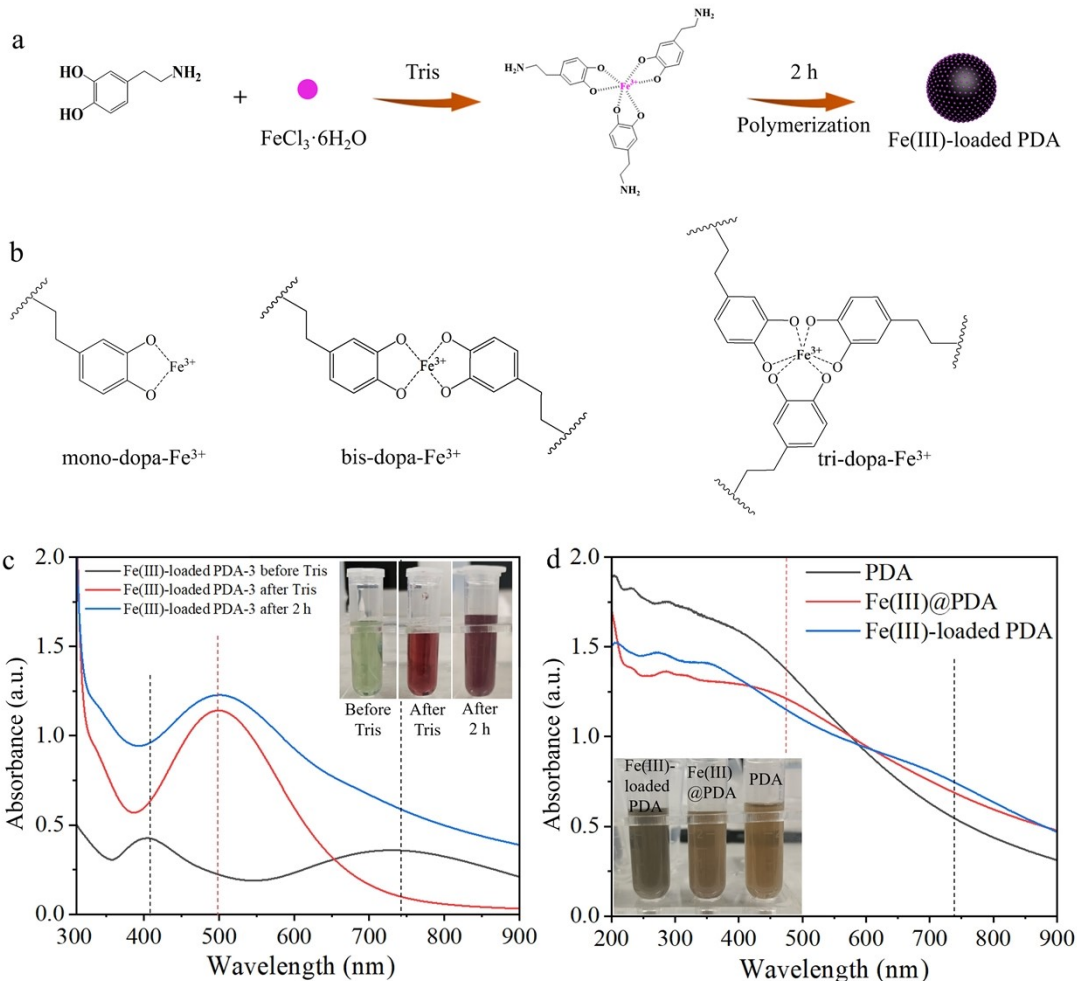


Figure S3. (a) Schematic illustration of the pre-doping strategy for preparing Fe(III)-loaded PDA. (b) Three existing forms of Fe-polydopamine complexes. (c) UV-Vis spectra of the solution before and after Tris addition, and after 2 h of Tris addition (inset: photographs of the solution before Tris addition, immediately after Tris addition, and after 2 h). (d) UV-Vis spectra of different products (inset: photographs of Fe(III)-loaded PDA-3, Fe(III)@PDA, and PDA after centrifugal washing, dispersed in water).

The complexes formed by the incorporation of Fe(III) ions into PDA have three existing forms: mono-dopa-Fe(III) ($\lambda_{\max} = 710$ nm), bis-dopa-Fe(III) ($\lambda_{\max} = 570$ nm), and tris-dopa-Fe(III) ($\lambda_{\max} = 490$ nm) complexes. The relationship between the coordination number and absorption peak position matched the theory well (Figure S3b).

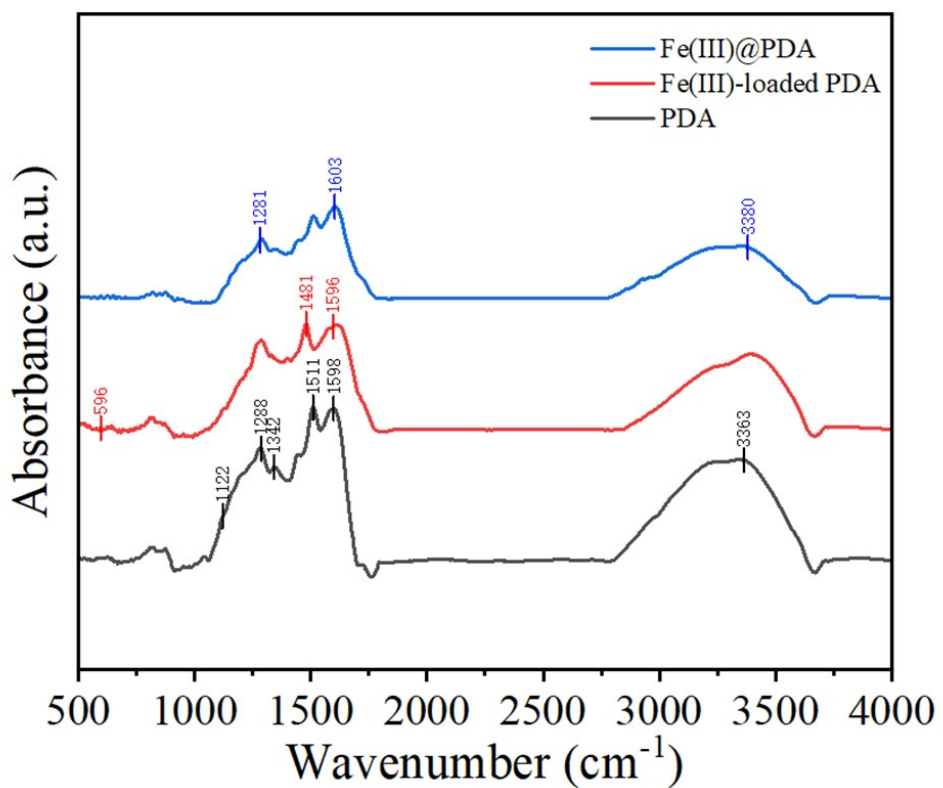


Figure S4. FTIR spectra of PDA, Fe(III)@PDA and Fe(III)-loaded PDA.

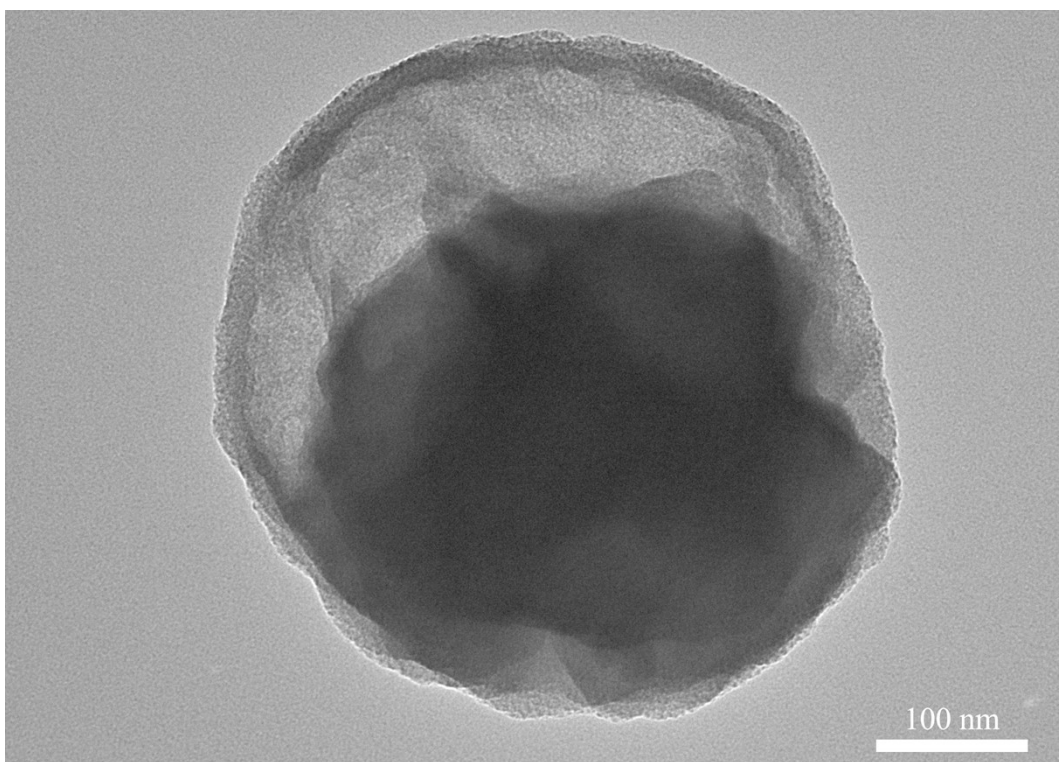


Figure S5. High magnification TEM images of Fe(III)@PDA@SiO₂-3.

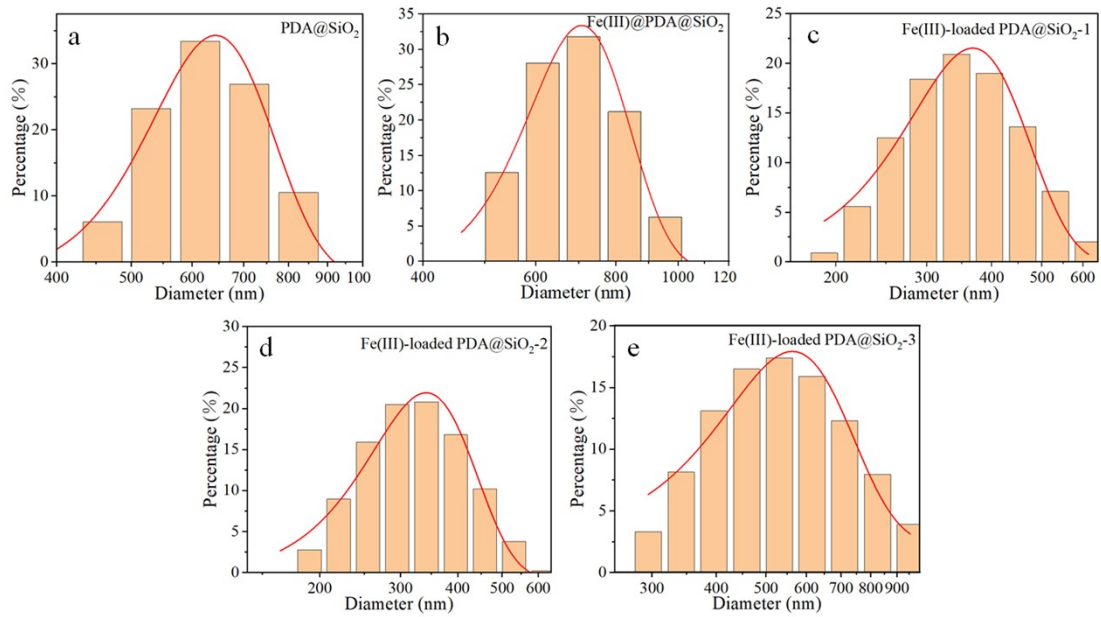


Figure S6. The diagrams of hydrodynamic particle size of (a) PDA@SiO₂, (b) Fe(III)@PDA@SiO₂, (c-e) Fe(III)-loaded PDA@SiO₂-(1-3).

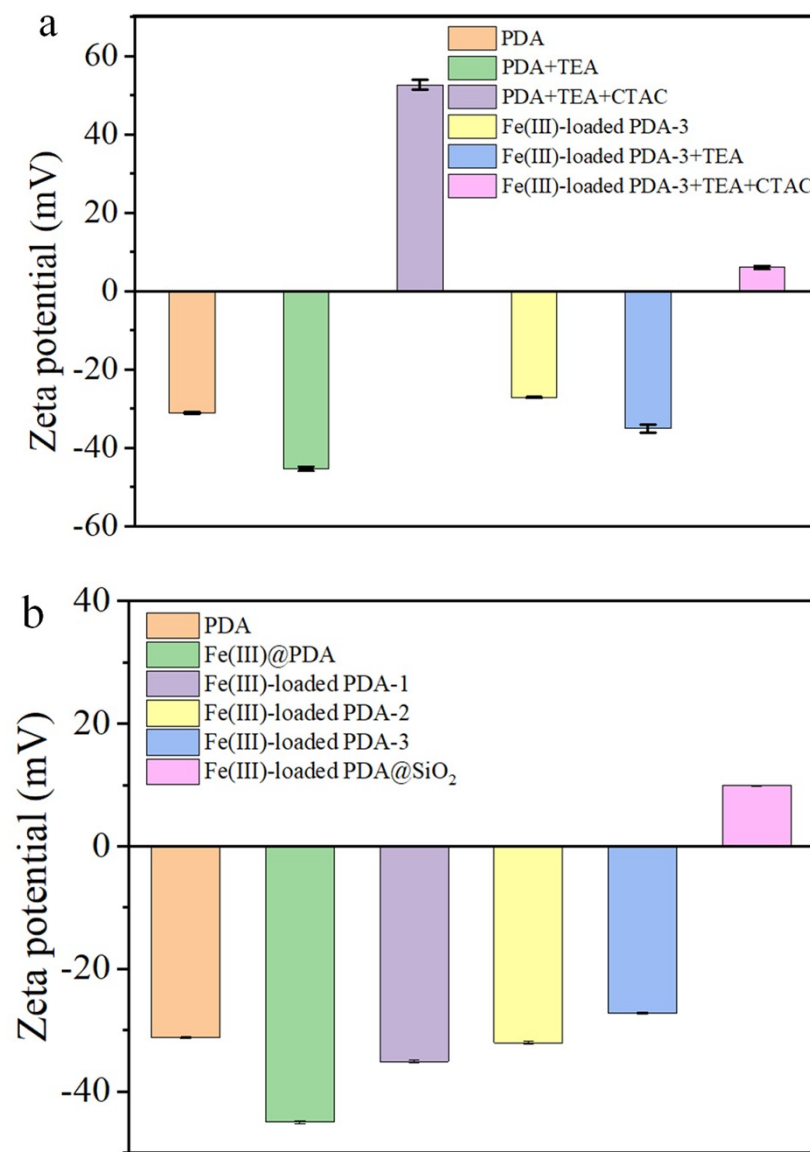


Figure S7. Zeta potential of: (a) PDA and Fe(III)-loaded PDA-3 before and after addition of TEA and CTAC, (b) PDA, Fe(III)@PDA, Fe(III)-loaded PDA-(1-3) and Fe(III)-loaded PDA@SiO₂-3.

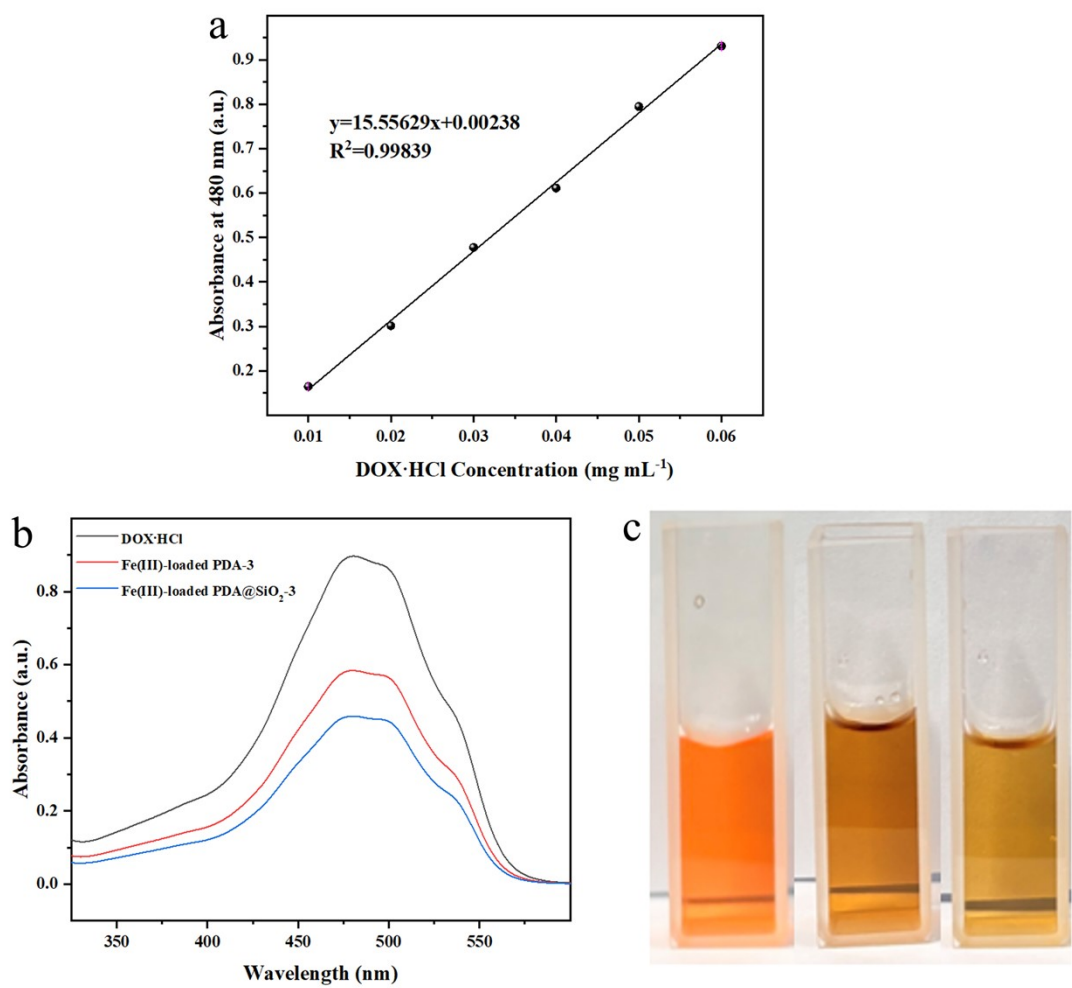


Figure S8. (a) Relationship of absorbance of DOX·HCl aqueous solutions at 480 nm wavelength depended on their concentration (mg mL⁻¹). (b) UV-vis absorption spectrum and (c) digital image of supernatants after adsorption of DOX·HCl aqueous solutions by Fe(III)-loaded PDA-3 and Fe(III)-loaded PDA@SiO₂-3.

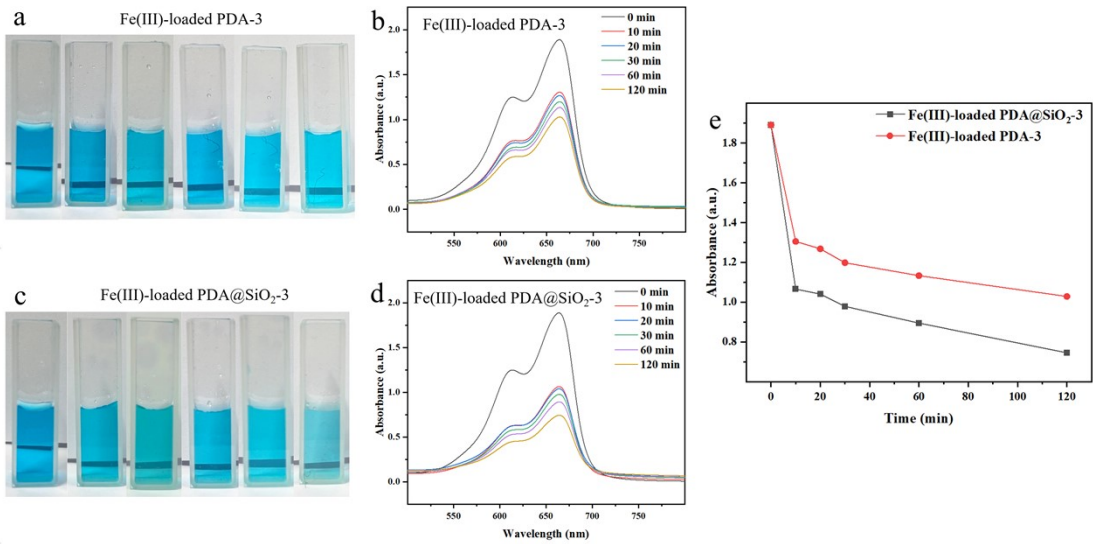


Figure S9. (a,c) Digital image and (b,d) UV-vis absorption spectra of supernatants after adsorption of MB aqueous solutions by (a,b) Fe(III)-loaded PDA-3 and (c,d) Fe(III)-loaded PDA@SiO₂-3. (e) Absorbance of MB aqueous solutions at 664 nm wavelength depended on time (min⁻¹) from (b,d) UV-vis absorption spectra.

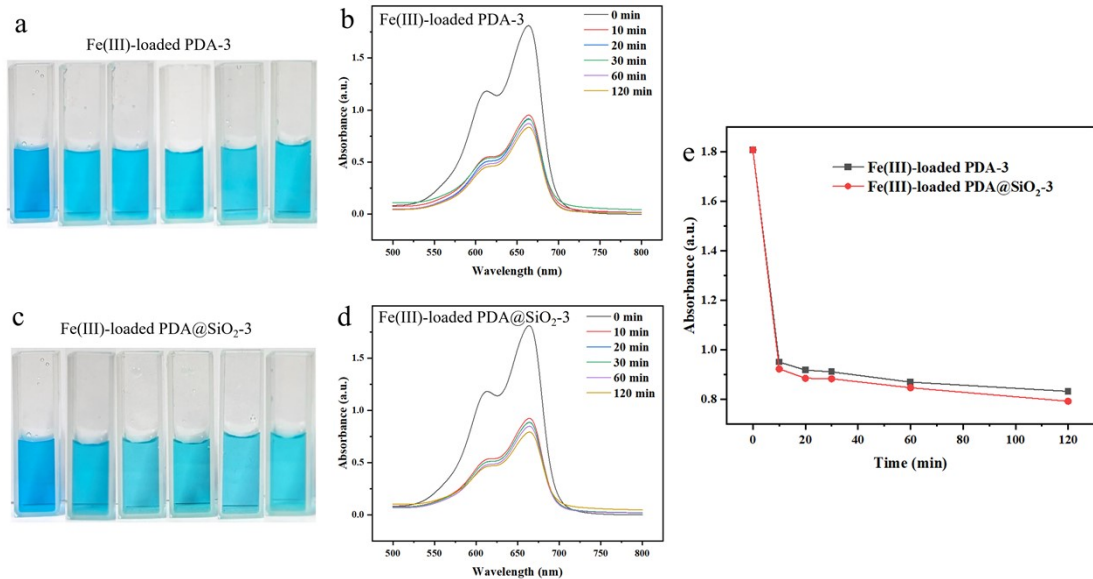


Figure S10. (a,c) Digital image and (b,d) UV-vis absorption spectra of supernatants after adsorption and catalysis of MB aqueous solutions by (a,b) Fe(III)-loaded PDA-3 and (c,d) Fe(III)-loaded PDA@SiO₂-3 under H₂O₂ (1.2×10^{-3} mM) condition. (e) Absorbance of MB aqueous solutions at 664 nm wavelength depended on time (min⁻¹) from (b,d) UV-vis absorption spectra.

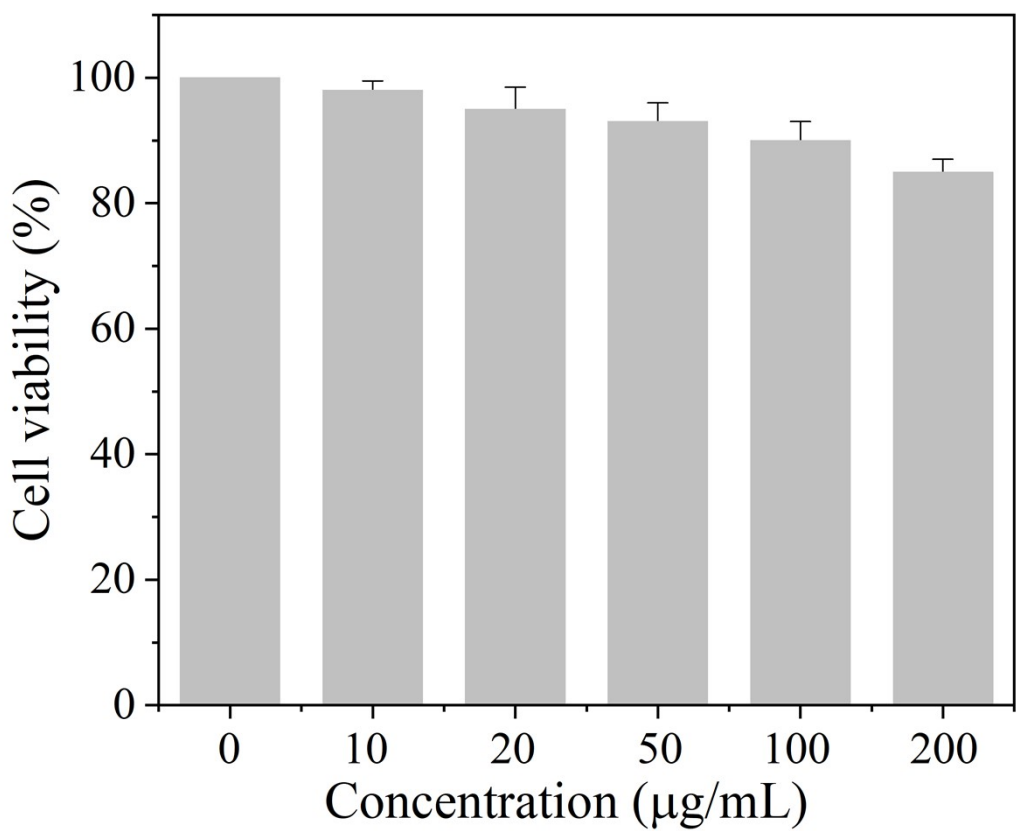


Figure S11. Cell viability of NIH/3T3 cells after incubating with different concentrations of Fe(III)-loaded PDA@SiO₂-3 (0, 10, 20, 50, 100, 200 $\mu\text{g mL}^{-1}$) for 6 hours.

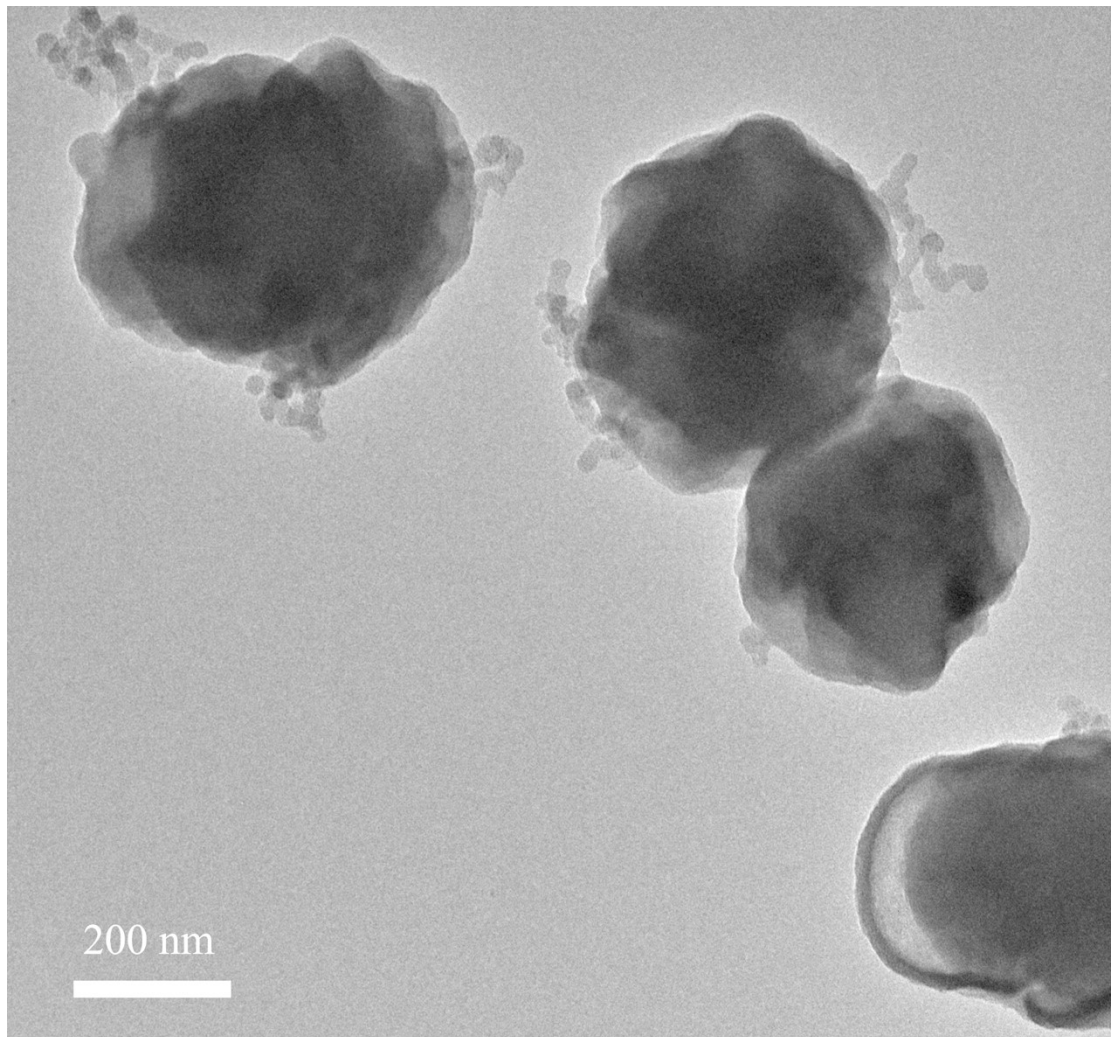


Figure S12. TEM image of Fe(III)-loaded PDA@SiO₂-3 after treatment in a tube furnace at 750 °C for 3 h under a constant N₂ flow.